

Anomalous temperature dependence in the Raman spectra of *l*-alanine: Evidence for dynamic localization

A. Migliori, P. M. Maxton, A. M. Clogston, E. Zirngiebl, and M. Lowe

Los Alamos National Laboratory, Los Alamos, New Mexico 87545

(Received 11 May 1988; revised manuscript received 4 August 1988)

We measured the temperature dependence of the intensity of the two lowest Raman modes in single crystals of *l*-alanine. The sum of the intensities obeys Maxwell-Boltzmann statistics accurately from 20 to 340 K but the intensities of the individual lines are anomalous. This behavior is explained by assuming that both lines share the same degrees of freedom but that a mode instability is triggered abruptly at an occupation of seven quanta. This instability, which has an activation energy of 500 K, is observed at temperatures as low as 20 K, possibly indicating the existence of dynamic localization of vibrational energy.

INTRODUCTION

The localization of vibrational energy in otherwise translationally invariant systems has received much theoretical attention. This localization, originally postulated by Davydov arises from the nonlinear interaction of optical phonons with acoustic phonons.¹⁻⁴ Recent theoretical work has suggested that interactions between optical phonons may also be significant.⁵⁻⁹ These theories propose that the self-trapping effects of a "softening" nonlinearity compete with the effects of dispersion resulting in envelope solitons which modulate the optical-phonon field. This dynamic localization breaks the translational symmetry of the system spontaneously without the intervention of impurities or defects. If nonlinear effects predominate, the system favors compact parcels of vibrational energy. If dispersion effects are strong in at least one direction, as is common for optical modes in systems with high symmetry, then localization is less favored and any localized state that does form will be broadly distributed (and thus difficult to distinguish from a harmonic, normal mode).

Localization of vibrational energy is known to occur in isolated molecules¹⁰ and in macroscopic systems¹¹ such as water waves and may occur in low-symmetry solids such as *l*-alanine. Theoretical studies^{1-9,12-15} of one-dimensional chains of molecular vibrators predict self-trapping of vibrational energy in strongly coupled vibrational fields where dispersion and nonlinearities are present, as is usual in actual systems. The nonlinearity can either be in the intervibrator coupling^{12,13,15} or in the single vibrator potential,¹⁴ the two cases representing significantly different physics. This sort of localization is distinct from localization associated with kinks which are topologically conserved, or charge which is absolutely conserved.¹⁶

Classical models of nonlinear chains and nonlinear continuous media¹¹ exhibit many types of stationary solutions. Some are periodic, all show localization to some degree, but only one is the classical soliton. There are, furthermore, nonstationary localized solutions with such a very small time dependence that in a nearly Hamiltonian

system they could not be differentiated from stationary states. Thus an observation of localization in a solid at low temperature is not equivalent to the observation of a soliton. However, the particular form of the localization is not particularly significant. Any of the stationary or nearly stationary solutions for the motion of a nonlinear dispersive system are excitations¹⁴ which could play a role in chemistry, energy transport,¹⁷ and other transport processes.

Hydrogen-bonded molecular crystals are appropriate systems in which to search for such effects. These crystals consist of discrete, relatively tightly bound molecular units held in position by highly nonlinear, relatively soft, hydrogen bonds. The dynamical optical spectra of these materials usually consists of high-frequency intramolecular modes and low-frequency lattice modes. The low-frequency lattice modes are likely candidates for soliton formation for several reasons. Because they are low-frequency modes, interaction with acoustic phonons is enhanced; the intramolecular modes allow for the possibility of Takeno-like interactions. Because they are the lowest-lying optical modes, fewer decay paths are available so lattice modes are more likely to be sufficiently long lived to make localization observable. In this paper, we report on some unusual behavior in the lattice modes of an orthorhombic molecular crystal, *l*-alanine, which may be interpreted as resulting from the dynamic localization of the lattice phonon field below 150 K.

MATERIAL

We chose to study the amino acid *l*-alanine for this work for several reasons. It can be grown from water solution as large colorless transparent single crystals so Raman spectroscopy is simplified. It is orthorhombic so that it satisfies the condition of low symmetry. Its lowest-frequency optical phonons are Raman active, IR inactive, so that complications from polaritons do not cloud the results. It has a positive thermal-expansion coefficient in the so-called *a* and *b* directions, and a small negative one in the *c* direction.¹⁸ Because all the interatomic potentials are known to have positive expansion

coefficients,^{19,20} the negative expansion coefficient can arise only from geometric effects associated with torsional motion coupling to longitudinal motion; thus the two strongly coupled fields required for localization are present. Its lowest optical modes are thermally populated below the melting point enabling temperature-dependent studies, and are known to have very long²¹ lifetime (> 1 ns). We note that *l*-alanine is a molecular crystal whose lowest-lying vibrational modes at 42 and 49 cm^{-1} have been the subject of several spectroscopic studies and molecular-dynamics simulations^{22–25} but, as these modes involve librations of the entire unit cell of a low-symmetry crystal, they have not been unambiguously assigned.

MEASUREMENTS

Seed crystals were prepared by thermally shocking a supersaturated solution of *l*-alanine in distilled, deionized water. Selected seeds were then grown to a final size of 4–9 mm by slow cooling or by slow evaporation of filtered saturated solutions. The best crystals were clear with few visible flaws. Crystal orientation was determined by known growth habits and confirmed by *x*-ray diffraction.

The Raman measurements were made on crystals held in place by a spring-loaded nylon clamp to the copper cold finger of a closed-cycle refrigerator. We used both the 488- and the 514-nm lines of an Ar^+ laser, with 514 nm giving the best signal to noise ratio. Incident power was varied from 50 to 200 mW with most data taken at 100 mW. The laser beam was incident along the *c* axis and polarized along the *b* axis. The scattered light was collected along the *a* axis and passed through a polarizer oriented along the *b* axis, $c(bb)a$, which maximized the intensity of the 42- cm^{-1} line at ambient temperature. Spectral observations were made with a scanning double monochromator. We scanned through the laser line for frequency calibration. Data were taken from 3 cm^{-1} up through the lines of interest, and also through an 851- cm^{-1} reference line for intensity calibration. The temperature, as measured on the cold finger, was varied from 5 to 323 K. We estimate from the data that ambient-temperature radiation and laser heating of the crystal and mount raised the sample temperature by approximately 15 K above that of the thermometer, and that this heating was a weak function of laser power. Other sources of error are estimated to be ± 10 K.

RESULTS

In Fig. 1 we show the Raman spectra of the lattice modes of *l*-alanine. The two lowest frequency modes are shown with higher resolution in Fig. 2.

In Fig. 3 we plot the Stoke's intensity versus temperature of the $42 \pm 0.4 \text{ cm}^{-1}$ and the $49 \pm 0.4 \text{ cm}^{-1}$ Raman modes. These data were normalized to the intensity of an 851- cm^{-1} mode which is expected to have an intensity independent of temperature for the temperatures of interest. All data were reduced using least-squares fits to Gaussians, with estimated relative intensity errors of

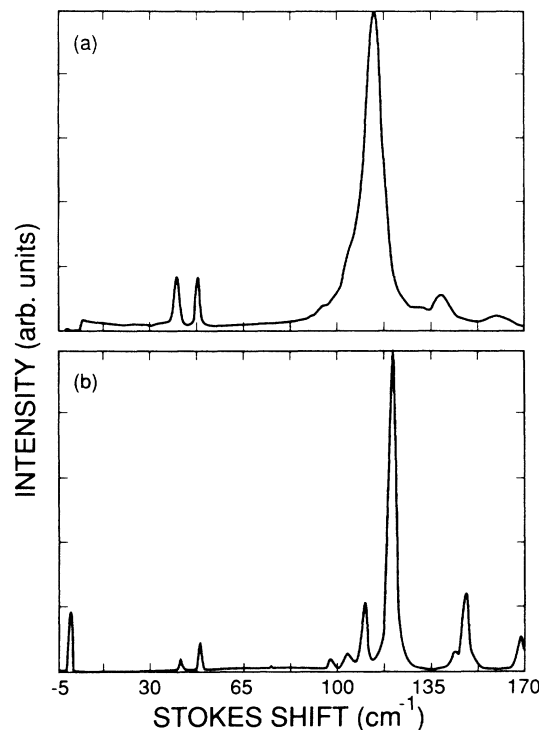


FIG. 1. Raman spectra of *l*-alanine at (a) 293 K and (b) 100 K.

$\pm 3\%$. We found that the sum of the intensities of the 42- and the 49- cm^{-1} lines, shown in Fig. 4, exhibited Maxwell-Boltzmann statistics (solid line in Fig. 4) to well within our expected errors. The only adjustable parameter was the small temperature error introduced by ambient and laser heating. The energy-level scheme for this

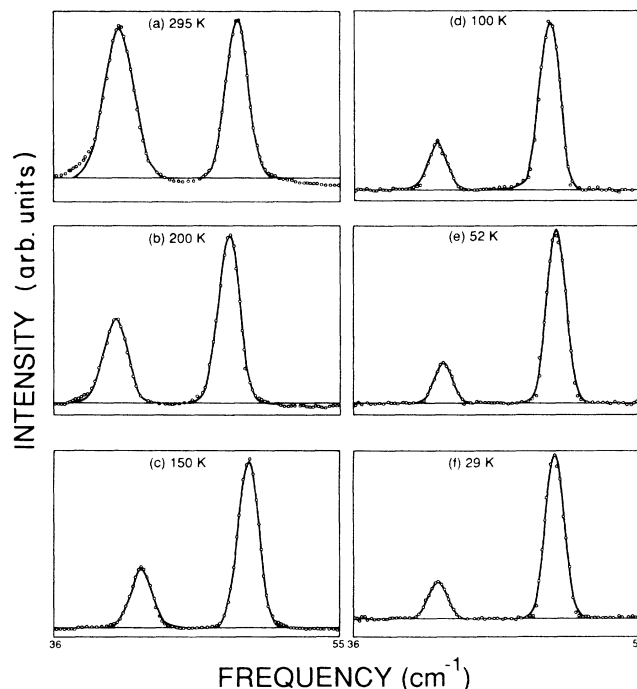


FIG. 2. High-resolution Raman spectra of 42- and 49- cm^{-1} peaks at various temperatures. Solid line is a Gaussian fit.

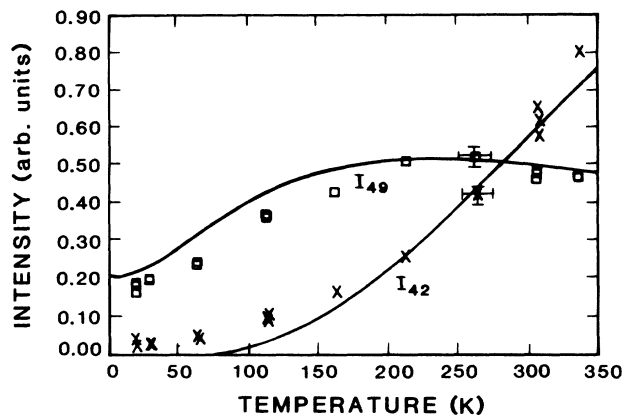


FIG. 3. Shown is the normalized intensity as a function of temperature for the 49-cm⁻¹ Raman mode (□) and the 42-cm⁻¹ Raman mode (×) in *l*-alanine. Also shown is the result of a model incorporating a mode instability (—). Typical error bars are shown on one data point.

Maxwell-Boltzmann fit was constructed with a spacing of E_1 between levels from the ground state to excited state m of a harmonic potential V_1 and a spacing of E_2 for a harmonic potential V_2 from level n up, suggesting that an instability occurs at m . The potential V_2 is assumed displaced from V_1 by a constant potential V . We conclude from this that the 49- and 42-cm⁻¹ lines are essentially the same degree of freedom. This energy-level scheme predicts the solid curves in Fig. 4. The intensities for the individual Stokes lines versus temperature, predicted by our model potentials, are

$$I_{49} = \frac{1}{N} \sum_{s=0}^{m-1} (s+1) e^{-(s+1/2)E_1/T}, \quad (1)$$

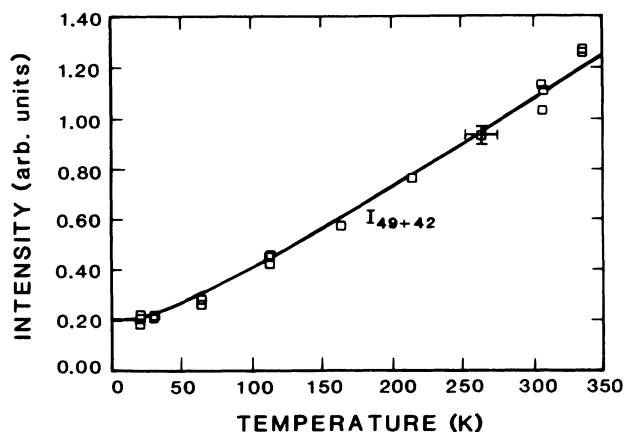


FIG. 4. Shown is the sum of the normalized intensities of the 42- and the 49-cm⁻¹ Raman modes (□) in *l*-alanine, and a Maxwell-Boltzmann distribution (—) for the energy-level scheme described in the text. Note that the sum of the intensities is Bose-like while the individual intensities are not. A Bose distribution for 45.5 cm⁻¹ is not detectably different from our solid curve.

$$I_{42} = \frac{1}{N} \sum_{s=n}^{\infty} (s+1) e^{-[(s+1/2)E_2+V]/T}, \quad (2)$$

where

$$N = \sum_{s=0}^{m-1} e^{-(s+1/2)E_1/T} + \sum_{s=n}^{\infty} e^{-[(s+1/2)E_2+V]/T}$$

and T is temperature in units of wave number. Using our measured values of $E_1=49$ cm⁻¹ and $E_2=42$ cm⁻¹ and the same temperature error found from the fit in Fig. 3, we then adjusted the parameters m and n in integer increments, and V . Our fit was very sensitive to m , and we found $m=7\pm 0.5$. Our sensitivity to n was lower, we found $n=9\pm 1$. Adding the parameter V , the constant offset between the potential having level spacing E_1 and the one having spacing E_2 did not improve the fit; the best choice was $V=0\pm E_1$. Also note that we observe no other Raman transitions below 49 cm⁻¹, down to our instrument limit of 3 cm⁻¹, supporting this value for V . This then is a fit with effectively one adjustable parameter n , because an integer step in m drastically degrades the agreement with the data, and V is small.

The curve drawn from Eq. (1) and Eq. (2) do not, however, fit the data so well below 150 K. The intensity deficit between the data and the model of the 49-cm⁻¹ mode reappears as a surplus in the 41-cm⁻¹ mode. In particular, the intensity of the 42-cm⁻¹ mode at 20 K would be less than our minimum detectable level if Eqs. (1) and (2) apply, but in fact it is about 100 times above what we can detect. If our energy level model represents the true physics of the system, we can interpret the discrepancy as follows. If nonlinear effects were not important, a normal-mode description would relate the appearance of the mode instability at $m=7$ ($E/k_b=500$ K) to a particular value of $\langle r^2 \rangle$, the mean-square displacement of the normal coordinate associated with this potential. So long as any spatial dependence of the vibrational motion is small on a scale of the lattice spacing, the correspondence between the mode instability and $\langle r^2 \rangle$ would be maintained. At high temperatures, it is likely that thermal effects associated with acoustic modes prevent any localization,¹³ hence only distributed thermal energy could produce a high enough vibrational level to reach the 42-cm⁻¹ threshold. At low temperatures, local modes could exist¹³ because the acoustic modes would have wavelengths much longer than a state localized over distances small compared to the wavelengths of optically generated phonons (< 2500 Å). The observation of the 42-cm⁻¹ vibration at low temperatures, then, cannot be caused by a normal mode because of the low level of excitation but it could result from a local mode characterized by regions of sufficient vibrational intensity to cross the 42-cm⁻¹ threshold. Thus the presence of a local mode could produce a failure of the normal mode description and lead to a Raman transition to a new state of localized vibrational energy at 42 cm⁻¹ above the ground state. It is this effect which can produce the excess 42-cm⁻¹ Raman intensity below 150 K.

Because the difference between the solid curves and the data in Fig. 4 appears to increase with temperature up to about 100 K and then decrease, it is likely that local

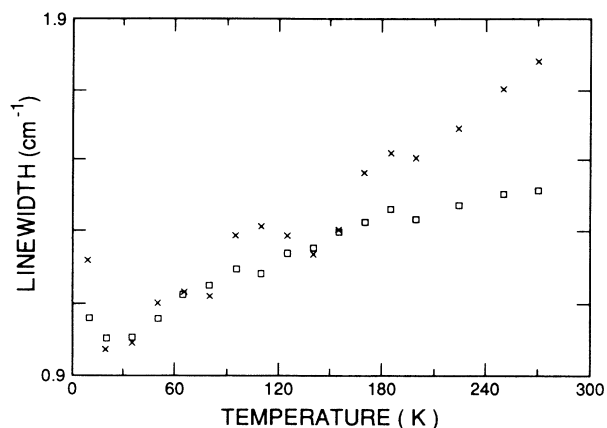


FIG. 5. Shown are the line widths full width at half maximum (FWHM) of the 49-cm^{-1} Raman mode (\square) and the 42-cm^{-1} Raman mode (\times) in *l*-alanine, as a function of temperature. Instrument resolution was approximately 1 cm^{-1} .

modes involving several quanta are also present and that these modes are accessed via both thermal and optical effects.

One should note that this localization is observable in this instance only as a result of the essentially fortuitous existence of the instability of the $49/42\text{ cm}^{-1}$ mode in *l*-alanine which produces an observable 7-cm^{-1} frequency shift. The intrinsic frequency shift occurring upon localization would in all probability be beyond the resolution of this experiment. While we acknowledge that dynamic localization is far from proven, this combination of instability plus localization, as a model, is thus far the only explanation we have found consistent with our experimental results.

We have considered such nonlinear effects as Fermi resonances in order to find alternative explanations for our results. However, for a Fermi resonance to produce

our measured temperature dependence, both a pathological Raman cross-section variation with temperature and a very strong and unexpected temperature variation of the potentials would be required. Other nonlinear effects are also hard to justify because we know that at low temperatures, coherent anti-Stokes Raman spectroscopy²¹ (CARS) measurements of lifetimes indicate that only one optically generated phonon is present at any given time. If any kind of temperature-dependent mode coupling were at work here we would expect an anomalous temperature dependence in the line widths. Figure 5 shows the line widths of the 42-cm^{-1} and the 49-cm^{-1} bands, determined by Gaussian fit, as a function of temperature; we see no evidence of mode coupling. We can rule out defect and impurity effects because of the large 42-cm^{-1} intensity at 20 K.

Although the data here are suggestive, clearly more work must be done to fully understand the Raman spectra of *l*-alanine. We are now in the process of using ultrasound, coherent anti-Stokes Raman scattering, isotopic substitution, and neutron scattering measurements to provide us with a more complete characterization. Of special importance is a determination of the full dispersion curve for the 49-cm^{-1} phonon. This will enable us to develop predictive models which can be used to further clarify this effect.

ACKNOWLEDGMENTS

The authors wish to thank I. Bigio, R. Bruinsma, Z. Fisk, P. S. Lomdahl, D. S. Moore, S. J. Putterman, D. S. Reagor, B. I. Swanson, and D. Schiferl for very valuable help of various sorts. We also wish to thank R. H. Heffner, S. S. Hecker, J. L. Smith, and D. Parkin for their support and encouragement. One of us (P.M.) wishes to acknowledge the support of Associated Western Universities. This work was carried out under the auspices of the U.S. Department of Energy.

¹A. S. Davydov, Phys. Status Solidi **30**, 357 (1963).

²A. S. Davydov, Phys. Ser. **20**, 387 (1979).

³A. S. Davydov, Zh. Eksp. Teor. Fiz. **78**, 784 (1980) [Sov. Phys.-JETP **51**, 397 (1980)].

⁴A. S. Davydov, Phys. Status Solidi B **59**, 465 (1973).

⁵S. Takeno, Prog. Theor. Phys. **69**, 1798 (1983).

⁶S. Takeno, Prog. Theor. Phys. **71**, 395 (1984).

⁷S. Takeno, Prog. Theor. Phys. **73**, 853 (1985).

⁸S. Takeno, Prog. Theor. Phys. **75**, 1 (1986).

⁹G. Careri, U. Buontempo, F. Galluzzi, A. C. Scott, E. Gratton, and E. Shyamsunder, Phys. Rev. B **30**, 4689 (1984).

¹⁰R. L. Swofford, M. E. Long, and A. C. Albrecht, J. Chem. Phys. **65**, 179 (1976).

¹¹A. Larraza and S. J. Putterman, J. Fluid Mech. **148**, 443 (1984).

¹²J. C. Eilbeck, P. S. Lomdahl, and A. C. Scott, Physica D **16**, 318 (1985).

¹³P. S. Lomdahl and W. C. Kerr, Phys. Rev. Lett. **55**, 1235 (1985).

¹⁴R. Bruinsma, K. Maki, and J. C. Wheatley, Phys. Rev. Lett.

57, 1773 (1986).

¹⁵D. Brown, B. West, and K. Lindenberg, Phys. Rev. A **33**, 4110 (1986).

¹⁶H. W. S. Treitwolf, Phys. Status Solidi B **127**, 11 (1985).

¹⁷J. C. Wheatley, D. S. Buchanan, G. W. Swift, A. Migliori, and T. Hofer, Proc. Natl. Acad. Sci. **82**, 7805 (1985).

¹⁸S. Forss, J. Raman Spectrosc. **12**, 266 (1982).

¹⁹F. A. Momany, L. M. Carruthers, R. F. McGuire, and H. A. Scheraga, J. Phys. **78**, 1595 (1974).

²⁰K. Machida, A. Kagayama, and Y. Kurada, Bull. Chem. Soc. Jpn. **54**, 1348 (1981).

²¹T. S. Koscic, R. E. Cline, and D. D. Dlott, J. Chem. Phys. **81**, 4932 (1984).

²²K. Machida and Y. Kuroda, Bull. Chem. Soc. Jpn. **54**, 1343 (1981).

²³C. H. Wang and R. D. Storms, J. Chem. Phys. **55**, 3291 (1971).

²⁴K. Machida, A. Kagayama, Y. Saito, and T. Uno, Spectrochim. Acta **34A**, 909 (1978).

²⁵J. Bandekar, L. Genzel, F. Kremer, and L. Santo, Spectrochim. Acta **39A**, 357 (1983).